



FRACTURE CRITERION FOR PREDICTING SURFACE CRACKING OF AA2017 ALLOY IN SEMI-SOLID FORMING PROCESS

^aCH Shashikanth and ^bG.Venkateswarlu ^cM. J. Davidson,

a Department of Mechanical Engineering, Sree Chaitanya College of Engineering, Karimnagar, Telangana, India-505527 , E-mail: shashikanth.chakunta@gmail.com

b Department of Mechanical Engineering, Sree Chaitanya College of Engineering, Karimnagar, Telangana, India-505527 , E-mail: ganta_hmp@rediffmail.com

^c Department of Mechanical Engineering, NIT Warangal, Telangana, India-506004 , E-mail: mj davidson2001@yahoo.co.in

* Corresponding Author: G.Venkateswarlu , Contact No.:91-9032194173
E-mail: ganta_hmp@rediffmail.com

Abstract:

AA2017 aluminium alloy billets were compressed till the appearance of crack on semi-solid compression tests conducted at 570^oC, 590^oC and 610^oC under strain rates of 0.16s⁻¹, 0.18s⁻¹, 0.2s⁻¹ to establish the fracture criterion during semi-solid forming process. The tests conditions were simulated in a finite element based simulation package DEFORM 2D. The critical damage factor based on Cockcroft and Latham algorithm were obtained by analyzing the results of the corresponding finite element calculation. The results show that the critical damage factor at different temperatures and strain rates is not constant but varying between 0.471 to 0.264. The Zener-Hollomon parameter which combines the effect of temperature and strain rate has been introduced in to the fracture criterion.

Keywords: solid forming, AA2017, FEM

DOI Number: 10.14704/NQ.2022.20.12.NQ77074

NeuroQuantology 2022;20(12): 925-936

1.0 Introduction

In any metal-forming process, the deformation will be done above the yield stress and care will be taken to limit the stress to within the failure stress. However, due to workhardening, the failure will be imminent and the successful prediction of the failure strain and stress will enable the industrial practitioner to design the process accordingly. Moreover, in the simulation studies, as the failure won't be visible, numerical failure criteria should be set in the simulation code to warn the user about the imminent failure. Thus, there is an essential requirement to predict and prevent fracture which is a major feature of the forming processes and thus the quality of the product. Most of the bulk deformation processes fail by ductile fracture due to the onset of internal or surface crack. In the semi solid process, the metal will be partly solid and partly liquid. However, at the end of the

deformation, the metal will be composed of more solid fraction with little or no liquid surrounding the solid metal. Thus, it is essential to incorporate the ductile failure based fracture criteria for semi solid forming processes with a limitation that the accuracy of the factor may vary at high liquid fraction even at the end of deformation. Several ductile fracture criteria have been reported in the literature, Freudenthal [1] used an effective stress and Cockcroft and Latham [2] employed maximum principal stress, respectively. On the other hand, there were approaches to utilize a combination between multiple stress components. Brozzo et al. [3] suggested a ratio between the maximum principal stress and maximum principal stress minus mean normal stress and Oyane [4] introduced a ratio between mean normal and effective stress. Also, there have been investigations to apply those criteria to various



processes and compare each other [5-7]. In the present work, the ductile fracture criteria for AA2017 aluminium alloy have been reported. The 2XXX series aluminium alloy has some advantageous properties like high strength at low specific weight, which makes them an excellent choice to use in the form of extrusion for aircraft fitting, wheels and major structural components [8-9].

The aim of the research work is to establish a fracture criterion for AA2017 alloy in the semi-solid state, capable of predicting the initiation of crack during the forming process and to optimize the processing parameters in such a way that the initiation of crack is delayed to avoided. For this purpose, a series of semi-solid compression tests were conducted over a wide range of process conditions in addition to finite element simulations. The procedure adopted and the critical damage factors found have been reported below.

2.0 Critical damage factor of AA2017 alloy based on Cockcroft and Latham damage

2.1. Cockcroft and Latham damage

The simulation part of the present work has been performed on DEFORM 2D, an FEA based simulation software. DEFORM predicts the initiation of crack using a critical value of Cockcroft Latham based algorithm. The critical damage factor is the critical value of the stress that causes failure of the metal due to the accumulation of stress leading to fracture. Cockcroft and Latham developed a damage computation module based on

cumulative damage theory that has been applied successfully to different loading conditions [8-9]. Cockcroft and Latham expressed damage in plastic deformation as an amount of work that the ratio of maximum tensile stress σ_T to effective stress σ_{eff} carries out through the applied equivalent strain ϵ_f in metal working process. It is given mathematically as

$$\int_0^{\epsilon_f} \frac{\sigma_T}{\sigma_{eff}} d\epsilon = C$$

(1)

Where ϵ_f is the total equivalent strain at the end of forming process. The magnitude of C cannot exceed a maximum value of C_{max} (critical damage factor) to failure. By comparison of C with C_{max} , the danger of material to failure throughout the process is estimated.

3.0 Experimental Procedure

AA2017 alloy with 15 mm diameter was used in this study. Its nominal chemical composition is 0.376 % Si, 0.345 % Fe, 3.33 % Cu, 0.66 % Mn, 0.65 % Mg, 0.180 % Zn, 0.034 % Cr, 0.076 % Ti, and 97.349 % Al (Wt %). Cylindrical specimens of 15mm diameter and 15mm in length were machined from a 16mm diameter rod. Compression tests at temperatures of 570°C, 590°C and 610°C and strain rates of 0.16 s⁻¹, 0.18 s⁻¹, and 0.2 s⁻¹ have been performed on a 50 ton hydraulic press. Samples were held at the test temperature for about 5 min and were upset till the onset of crack. Compressed sample with their microstructure are shown in Fig 1.



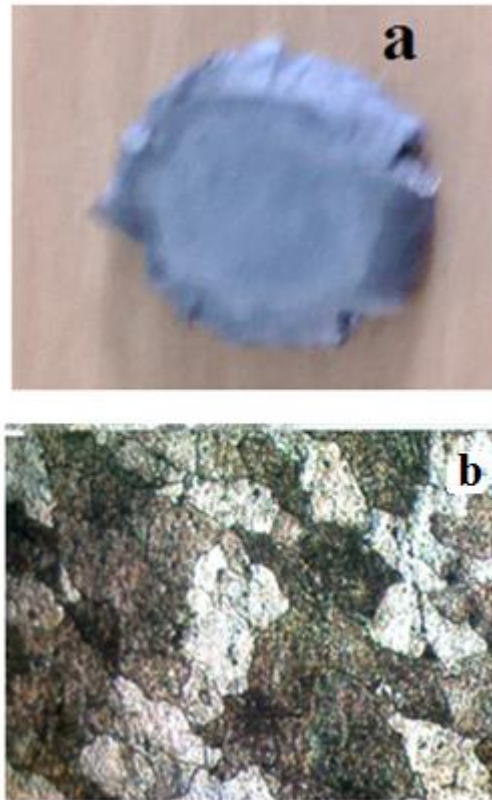


Fig.1 (a) Fracture samples and (b) Microstructures with internal cracks at temperatures at 570°C

4.0 Results and discussion

4.1 Determination of critical damage factor for AA2017 alloy

The critical value of the damage factor depends on the mechanical and metallurgical state of the metal before and after the deformation process. As such, the factors such as the initial microstructure, alloy constituents, grain size, grain form, non-metallic inclusion content, hardness etc affect the critical damage factor and they are different for different initial and final conditions. In the present work, as the temperature, strain rate and solid and liquid contents change during the deformation process, these are the critical factors that affect the damage factor. In order to predict the incidence of surface fracture, the value of the Cockcroft-Latham equation expressed by means of Eq.(1) has been calculated for the different process condition chosen in the

present investigation. Moreover, as the damage factor is calculated based on the cumulative damage theory, the damage value just before and deformation step will be lesser than the current step and it will increase progressively till a critical value, beyond which the actual failure of the metal will happen. This progressive increase of damage factor has been assessed by calculating a incremental damage ratio (I_{DR}) given by the formula

$$I_{DR} = \frac{\Delta D}{D_{accum.}} \quad (2)$$

Where $I_{DR} = \Delta D / D_{accum.}$ is the ratio of the damage increment at a particular step (ΔD) to the immediately next step (accumulated value) ($D_{accum.}$) [10].

The damage factor was retrieved from the simulation data up to the onset of failure. The simulation was performed by giving the

true stress strain curve generated from the experiments as input in the constitutive relation. The incremental damage ratios have been calculated from the simulation till the onset of fracture and have been plotted in Fig 2-3. Fig. 2 shows the damage distribution at last step (height reduction of 70%) at 570°C and strain rate of 0.16s⁻¹. From the simulation results, it is found that the maximum damage value is found in the edge of the disc sample and it is minimum in the middle of the disc. As the deformation starts from the middle and progresses towards the edge, the metal that was deformed a little

while ago in the middle will be pushed away from the centre towards the periphery and fresh metal from the height side of the sample will be pushed towards the centre. Thus, with each step, fresh metal will be deformed and will be pushed towards the edge. Thus, a deformation gradient would have been formed from the centre to the edge. The metal at the edge would be the metal that has deformed more and thus would have undergone more workhardening. This is the reason for fracture to initiate at the edge first and also for its highest damage factor.

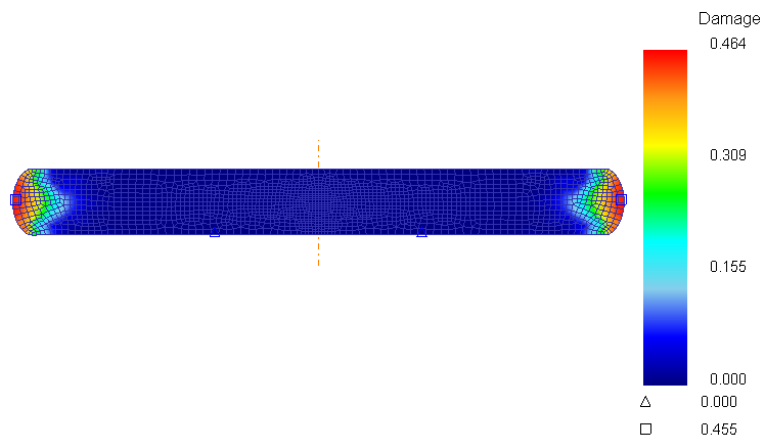
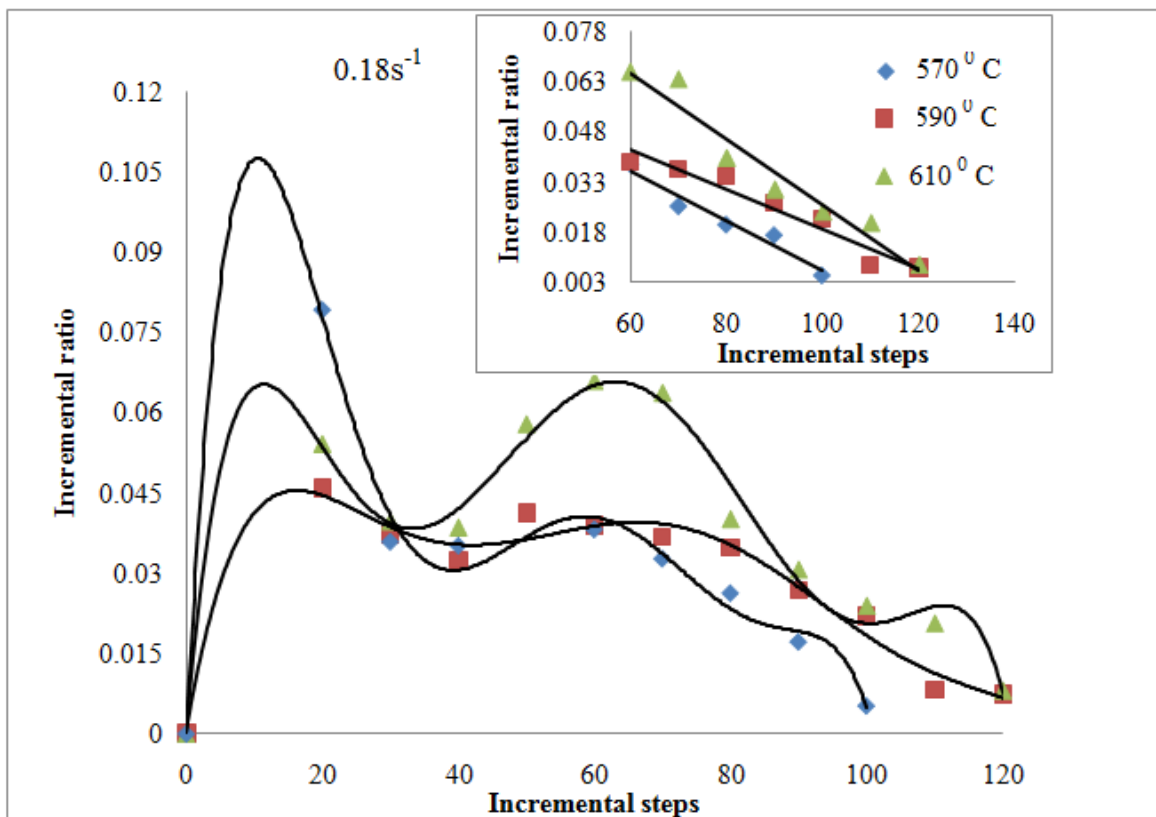
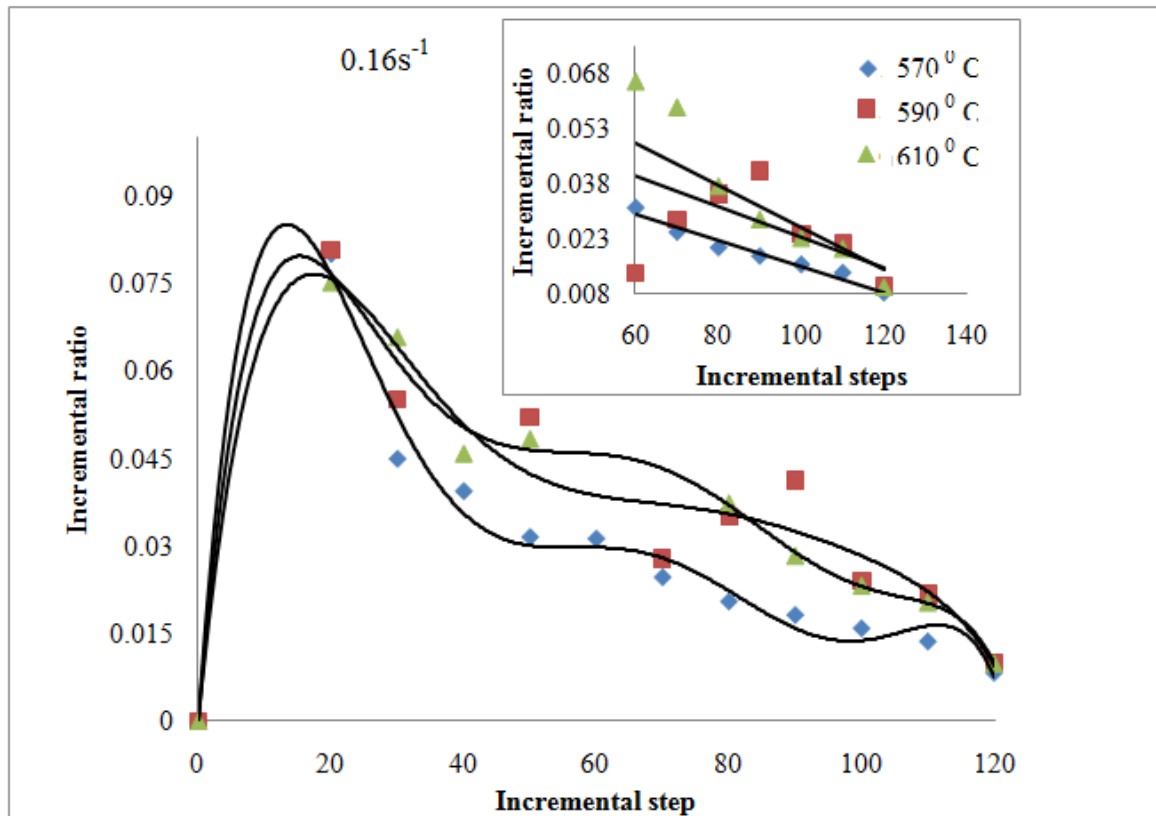


Fig. 2 Damage distribution at last step (height reduction of 70 %) at 570°C and strain rate of 0.16 s⁻¹.

Fig.3 shows the variations in the incremental ratio during the compression process at different temperatures and strain rates. The inset shows the variation if the incremental ratio after 60 steps. It can be seen that I_{DR} decreases to trough point rapidly, then it has a slight increase, soon after it decreases to zero gradually. To know the fracture time (step), the point arrays after step 60 are taken from each incremental ratio varying curve and fitted linearly as shown in Fig. 3.





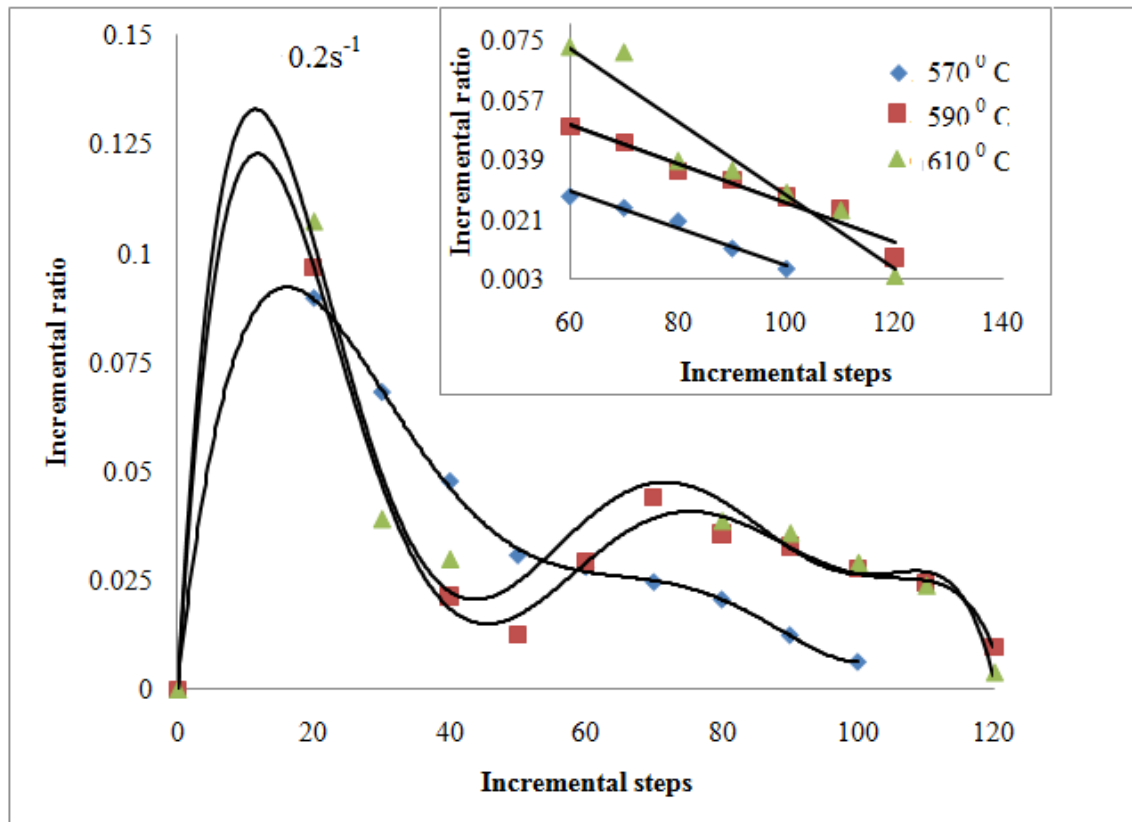


Fig.3 Variation of Incremental ratio of Cockcroft-Latham damage during compression process at different temperatures and different strain rates.

The maximum cumulative damage value at last step or the critical damage factor is obtained. In this way, the critical damage factor of AA2017 alloy was computed.

4.2 Effect of Strain rate and temperature on damage values

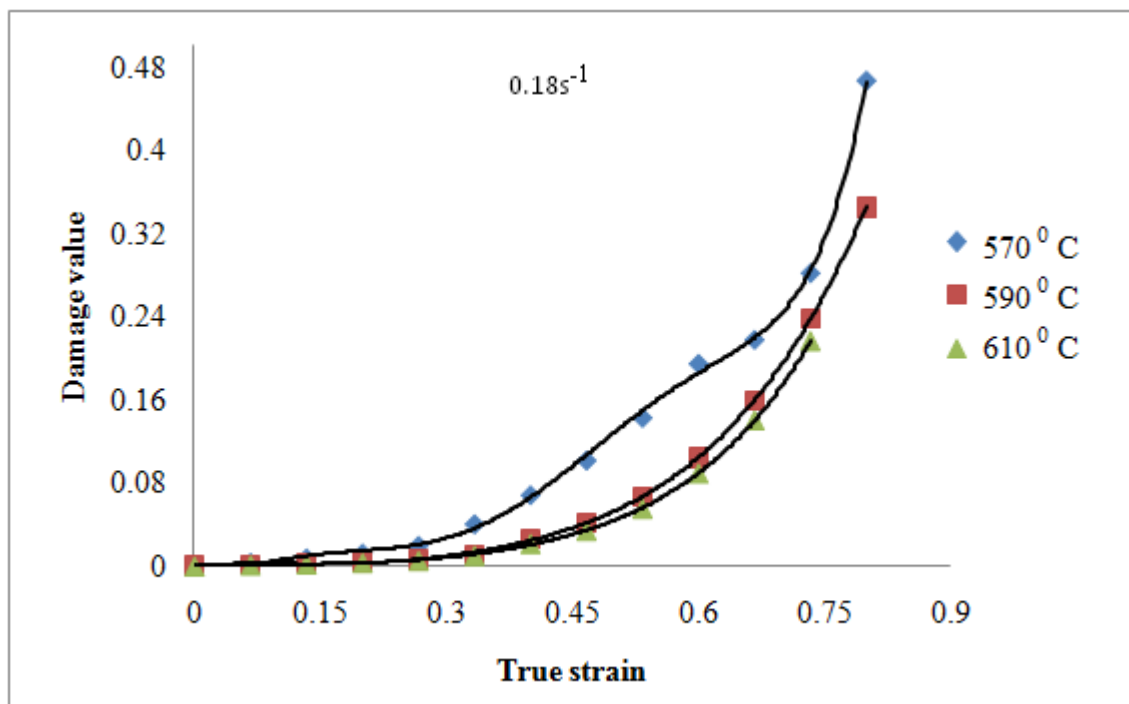
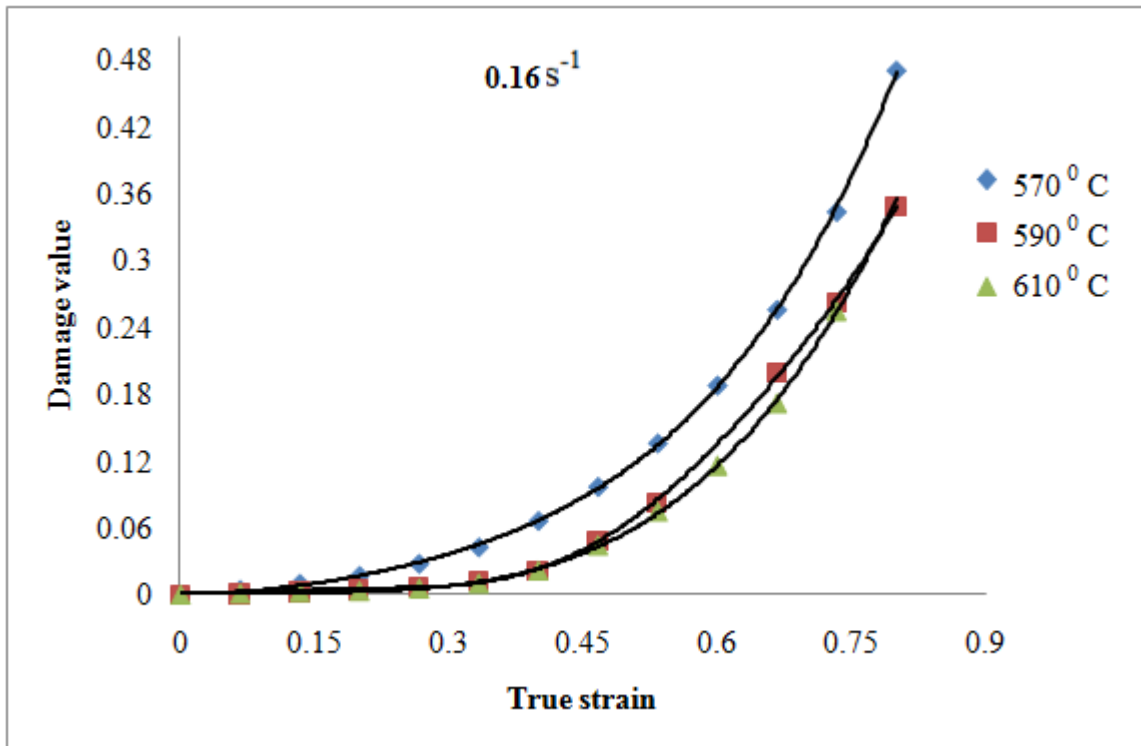
The critical damage factor at 570°C, 590°C and 610°C and at strain rates of 0.16, 0.18 and 0.2 s⁻¹ are given in Table 1. The critical damage factor varies from 0.471 to 0.264. Further, the critical damage value decreases significantly with increase in strain rate.

Table 1. Critical damage factor at different temperatures and strain rates.

Strain rate	570°C	590°C	610°C
0.16 S ⁻¹	0.471	0.349	0.379
0.18 S ⁻¹	0.467	0.345	0.370
0.20 S ⁻¹	0.455	0.337	0.264

Fig. 4 shows the variation of damage factor value with the true strain. It can be seen that the damage increases non-linearly as the compressive true strain increases from 0 to 0.5, and then it increases nearly linearly. Comparing the results with one another, it is found that for fixed true strain the maximum cumulated damage decreases with increasing of temperature.





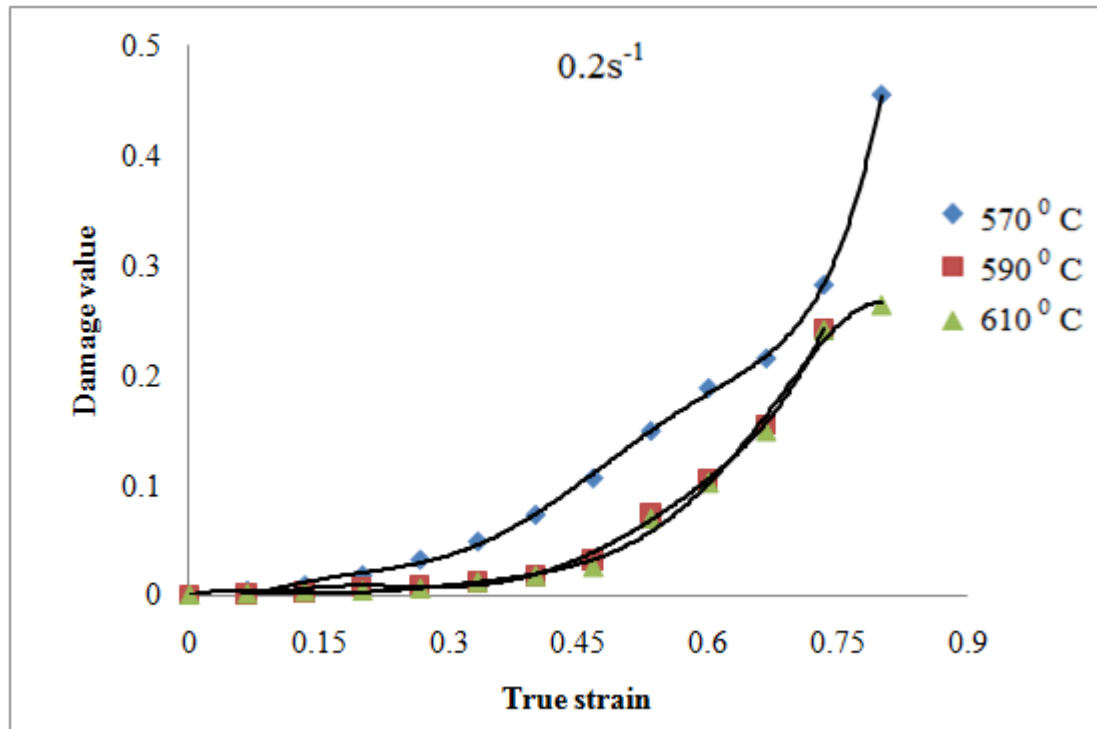


Fig. 4 Variation of damage value with true strain during compression process at different temperatures and strain rates.

4.3 Constitutive Model for Hot Forming

At high temperature, the deformation is controlled by a thermal activation method. Sellars [11] stated that the steady-state flow stress of the thermal deformation depends on the deformation temperature and also on the strain rate, which might be expressed by the equation;

$$\dot{\epsilon} \exp\left(\frac{Q}{RT}\right) = Z = A (\sinh(\alpha\sigma))^n \quad (3)$$

Where Z is the temperature compensating strain rate factor, i.e. the Zener-Hollomon parameter; $\dot{\epsilon}$ is the strain rate; Q is the deformation activation energy; σ is the steady state flow stress; R is the gas constant, $8.31 \text{ J} \cdot \text{mol}^{-1} \cdot \text{K}^{-1}$; and T is the temperature. The material constants such as A, α , β , and n, where ' α ' the stress multiplier, 'n' the stress exponent, 'A' and ' β ' the material constants, have been evaluated by performing disc compression tests at temperatures of 570°C, 590°C, and 610°C and strain rates of 0.16, 0.18, and 0.2 s^{-1} [12]. Fig. 6 shows the relationship between critical fracture strain C_s and $\ln Z$. A linear relationship was observed between these two. This means that fracture is mainly controlled by $\ln Z$ rather than by temperature and strain rate separately. A regression equation containing the critical fracture strain has been computed and is given in Eq. (4).

$$C_s = 23.885 - 1.787 \ln Z \quad (4)$$



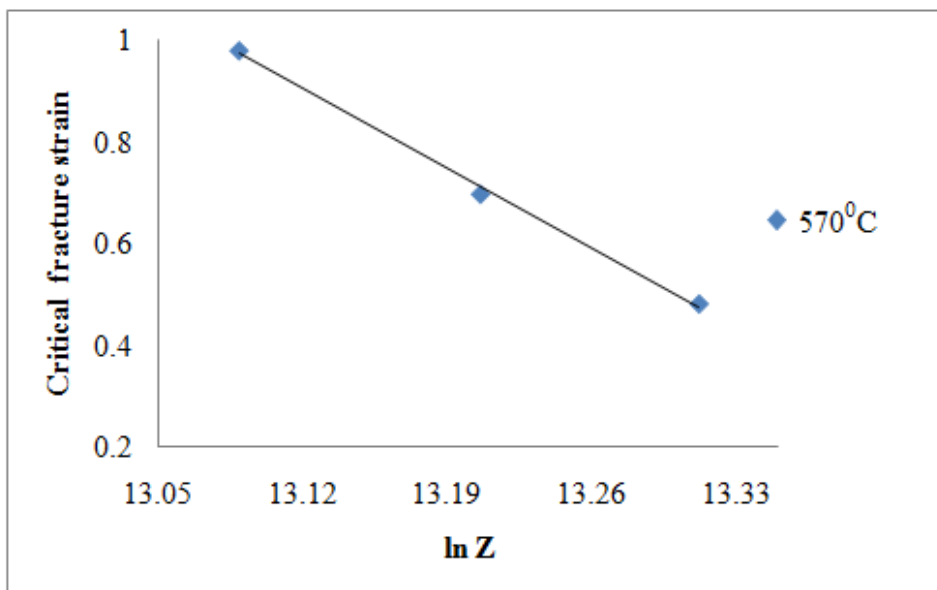


Fig. 5 Fracture strain as function of ln Z and temperature

4.4 Zener-Hollomon based fracture parameter for AA2017 alloy at semi-solid forming

Fig.6 shows the relation between the critical fracture value C_f and ln Z. A linear relationship is seen between C_f and ln Z. Its regression equation is given by

$$C_f = 3.20 - 0.214 \ln Z \tag{5}$$

The correlation coefficient is 0.9072. The regression line is seen as a boundary separating the safe and the unsafe regions. If the damage value at any particular simulation step falls within the regression line, it is considered safe forming and the damage value that crosses the regression line implies that failure has actually taken place. Taking the above into consideration, the Cockcroft and Latham can be written in the form shown below [13]

$$C > C_f \tag{6}$$

$$\int_0^{\epsilon_f} \frac{\sigma_T}{\sigma_{eff}} d\epsilon > 3.20 - 0.214 \ln Z \tag{7}$$

Eq. 7 is the fracture criterion of AA 2017 alloy in the semi-solid forming process. The left hand side is the damage that the material exhibits during the plastic deformation at any particular strain value and the right hand side is the critical fracture value. The equation of the above form involves the role of temperature compensated strain value for damage calculation, thus relating the forming temperature and strain rate in the damage parameter.



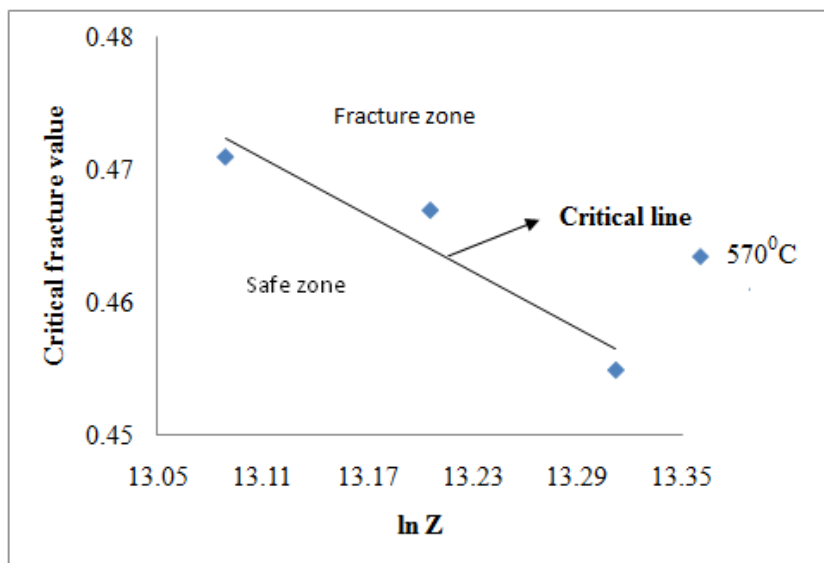
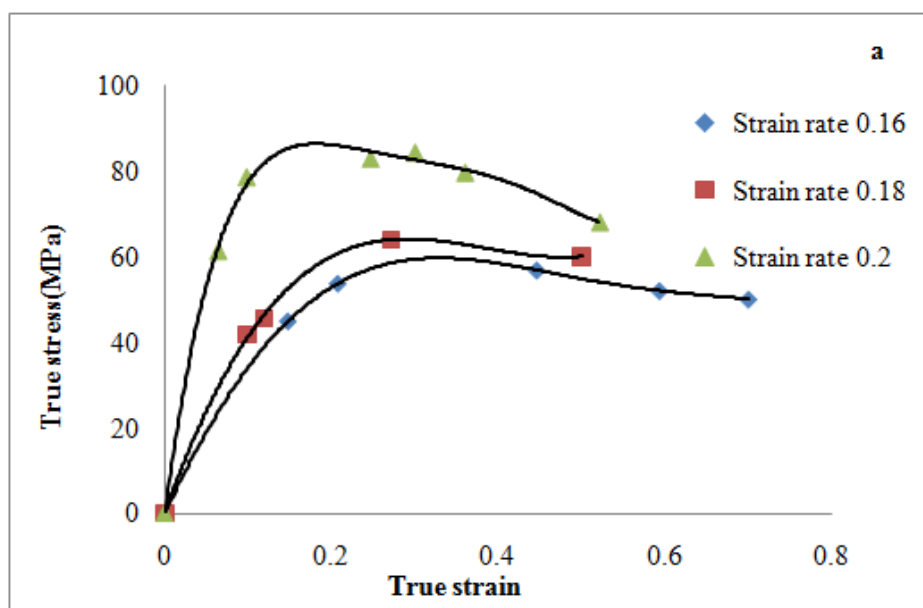


Fig.6 Relation between ln Z and critical fracture value, C_f

4.5 True stress-true strain curves

The true compressive stress-strain curves of AA2017 alloy are shown in Fig.7. The flow stress and the shape of the flow curve dependent largely on the temperature and strain rate. For all of the specimens, the stress of the specimens increased initially and then dropped down due to recrystallization and softening mechanism. The softening mechanism was experienced for different strain rates and temperatures.



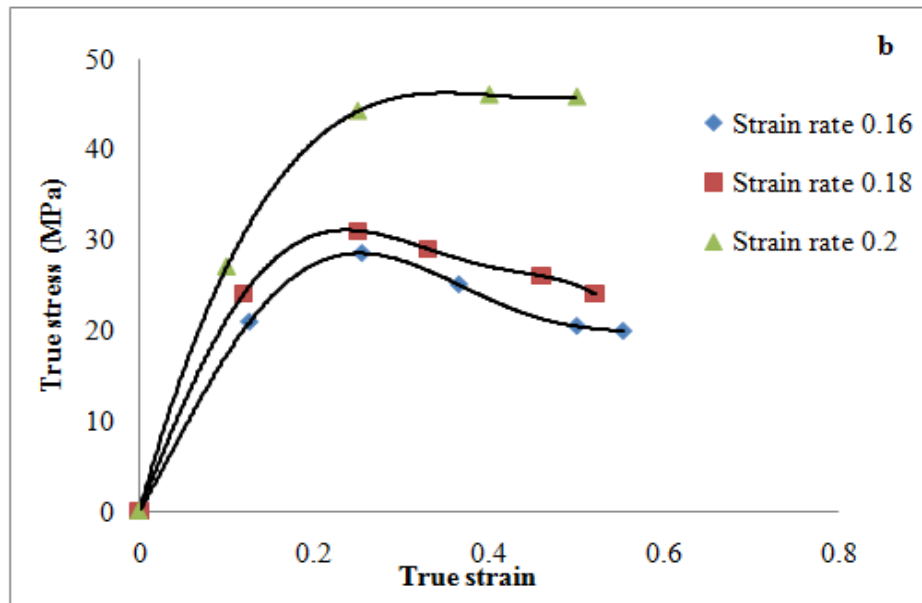


Fig.7 Compressive True stress-True strain curves at different temperatures of (a) 570°C and (b) 610°C

5. Conclusion

In the present work, the critical damage factor of AA 2017 alloy based on Cockcroft and Latham equations was found and it was observed that the critical damage value is not a constant but varying in between 0.471 to 0.264. It decreases significantly with the strain rate and it increases with temperature. It can be seen that the damage increases non-linearly as the compressive true strain increases from 0 to 0.5, and then it increases nearly linearly. The progression of damage with deformation has been identified and the critical damage for different temperatures and strain rates has been calculated. These damage factors can be used by the users of semi solid forming process for setting the forming limits at simulation studies.

References:

- 1) A.M Freudenthal. The inelastic behaviour in solids, First Edition. New York: Wiley; 1950.
- 2) MG. Cockcroft, DJ. Latham. Ductility and workability of metals. Journal of the Institute of Metals 1968; 96:33-39.
- 3) P Brozzo, B Deluka, R Rendirina. A new method for the prediction of formability in metal sheets. Proceedings of the 7th Biennial Conference of the International Deep Drawing Research Group 1972:9-13.
- 4) M. Oyane. Criteria of ductile fracture strain. Bulletin of the JSME 1972; 15:1507-1513.
- 5) SE Clift, P Hartley, CEN Sturgess, GW Rowe. Fracture prediction in plastic deformation processes. International Journal of Mechanical Sciences 1990; 32:1-17.
- 6) AS Wifi, A, Abdel-Hamid, N El-Abbasi. Computer-aided evaluation of workability in bulk forming processes. Journal of Materials Processing Technology 1998; 77:285-293.
- 7) HS Kim, YT Im, M Geiger. Prediction of ductile fracture in cold forging of aluminium alloy. Journal of Manufacturing Science and Engineering 1999; 121:336-344.
- 8) I. J. Polmear: 'Light alloys.' metallurgy of the light metals'; 1996[2], London, Halsted Press. ASM Metal Handbook. Vol.2



- 9) J. E. Hatch: 'Aluminium properties and physical metallurgy'; 1984, Materials Park, OH, ASM.
- 10) XIA Yu-feng, QUAN Guo-zheng, ZHOU Jie. "Effects of temperature and strain rate on critical damage value of AZ80 magnesium alloy". Transactions of Nonferrous Metals Society of China
- 11) C.M. Sellars. Materials Science and Technology, 1 (1985) 325 .
- 12) C.H. Shashikanth and M. J. Davidson, "Simulation studies on deformation behaviour of AA 2017 alloy in the semi-solid state using FEA", Materials at high temperature, 2014, 31, 3.
- 13) ZHANG Xue-min, ZENG Wei-dong¹, SHU Ying , ZHOU Yi-gang, ZHAO Yong-, WU Huan, and YU Han-qing, "Fracture criterion for predicting surface cracking of Ti40 alloy in hot forming processes", Transactions of Nonferrous Metals Society of China, 2009(19), 267-271.

